

Microscopically-resolved simulations prove the existence of soft cluster crystals

Dominic A. Lenz,¹ Ronald Blaak,¹ Christos N. Likos,¹ and Bianca M. Mladek²

¹*Faculty of Physics, University of Vienna,
Boltzmanngasse 5, A-1090 Vienna, Austria*

²*Department of Structural and Computational Biology,
Max F. Perutz Laboratories GmbH, University of Vienna,
Campus Vienna Biocenter 5, A-1030 Vienna, Austria*

(Dated: August 31, 2021)

Abstract

We perform extensive monomer-resolved computer simulations of suitably-designed amphiphilic dendritic macromolecules over a broad range of densities, proving the existence and stability of cluster crystals formed in these systems, as predicted previously on the basis of effective pair potentials [B. M. Mladek *et al.*, Phys. Rev. Lett. **96**, 045701 (2006)]. Key properties of these crystals, such as the adjustment of their site occupancy with density and the possibility to heal defects by dendrimer migration, are confirmed on the monomer-resolved picture. At the same time, important differences from the predictions of the pair potential picture, stemming from steric crowding, arise as well and they place an upper limit in the density for which such crystals can exist.

PACS numbers: 82.70.-y, 82.30.Nr, 64.70.D-, 83.10.Tv

Soft cluster crystals (also termed bubble solids), i.e., solids where each lattice site is occupied by several, interpenetrating particles, arise in systems governed by generic, *purely repulsive* interactions which remain *finite* even if particles fully overlap [1–3]. The completely different character of these novel cluster crystals, as opposed to hard cluster phases [4, 5], is testified by the fundamentally distinct nature of the interactions between their constituent particles. The clusters are not stabilized by a combination of short-range attractions and long-range repulsions, which result in well-defined aggregates in the liquid that disappear at high densities [4, 5]. Rather, clustering is here a self-enhancing, cooperative phenomenon, where full overlaps with few particles are favored over costly partial overlaps with many neighbors. Thus, clusters remain stable due to their mutual repulsions with the surrounding ones [6]. Cluster crystals are thus high-density phases, in which fuzzy agglomerates, already formed in the liquid, freeze into well-defined and spatially ordered groups at higher concentrations [3]. Predicted for certain macromolecular [1, 2, 8] or atomic [10–13] systems, such clusters form exotic crystals that show mass transport [14, 15], unusual reaction to compression [3, 6, 16] and shear [17], and rich phase behavior with a cascade of isostructural transitions [18, 19]. Further, they possess a unique rheological behavior, showing thixotropy and flow quantization [17].

All hitherto performed studies of the properties of soft cluster solids have been based on the assumption of ultrasoft, *pairwise additive*, *density-independent* inter-particle interactions. According to theory, the necessary requirement for a system to display clustering behavior is that its pair interaction shows negative Fourier components [2, 20]. The pair potential picture is realistic when understood as an effective representation of certain types of polymeric macromolecules in *not too concentrated* solutions [21–23]. However, the relevance of such an approach for experiments is here put into question since the formation of clusters is a high density phenomenon. Under such conditions, many-body effects, conformational deformations and crowding are expected to play a crucial role, which could either hinder or favor cluster formation. For ring polymers, the zero-density pair interaction has negative Fourier components; however, due to the shrinkage of the rings at finite densities, the clustering ability is lost [8]. In this Letter, we show on a microscopic basis that soft cluster crystals can indeed be stabilized in a broad density regime for suitably designed macromolecular systems, motivating the experimental realization of such systems.

Amphiphilic dendrimers constitute such a system predicted to show clustering [1, 2].

Here, we consider amphiphilic dendrimers of second generation with two central monomers. The dendrimers' 14 monomers are divided into two classes: the eight outermost monomers form a solvophilic shell which surrounds the solphophobic core build from the interior generations' monomers. At sufficiently close separations, all monomers strongly repel each other via Morse potentials, while bonds between monomers are modeled by FENE springs [24]. In previous studies, the zero-density effective pair interaction between various realizations of such dendrimers has been determined [1], showing the desired negative Fourier components [25]. Indeed, we then found the onset of clustering in the *fluid* phase of *microscopically-resolved* amphiphilic dendrimers [2]. Here we demonstrate the stability of the cluster solid phase (see scheme in Fig. S1 of the Supplemental Material). Let $\rho = N/V$ be the density of a system of N dendrimers in the volume V and R_g be the $\rho = 0$ radius of gyration of such a dendrimer. An estimate, $\tilde{\rho}_f$, of the freezing density ρ_f can be obtained on the basis of the infinite dilution pair potential $\Phi_{\text{eff}}(r)$ [20]. Further, theory predicts the number of dendrimers per cluster, i.e., the occupancy \tilde{N}_{occ} , to be proportional to the density: $\tilde{N}_{\text{occ}} \propto \rho$ [2, 3]. Consequently, the lattice constant $\tilde{a} \propto (\tilde{N}_{\text{occ}}/\rho)^{1/3}$ is predicted to be density-independent. For the dendrimers considered here, lattice site occupancies of $\tilde{N}_{\text{occ}} = 3.5$ (bcc) and $\tilde{N}_{\text{occ}} = 3.2$ (fcc) are predicted at the freezing density $\tilde{\rho}_f R_g^3 = 0.281$. The lattice constants are predicted as $\tilde{a} = 2.9R_g$ (bcc) and $\tilde{a} = 3.6R_g$ (fcc), leading in both cases to nearest-neighbor distances $\tilde{d} = 2.5R_g$.

These theoretical predictions are put to the test by performing NVT-Monte Carlo simulations. First, we delimit the range of values of N_{occ} that can stabilize crystals: although in the effective description N_{occ} can be arbitrarily large, in the monomer-resolved description local steric crowding is anticipated to put an upper limit to this quantity. To this end, we simulate *disordered* systems of dendrimers in a density regime around $\tilde{\rho}_f$. We study the cluster size probability distribution $P(N_{\text{occ}})$, employing a cluster algorithm developed previously [2]. Representative results are shown in Fig. 1 for three different densities. Fig. 1(a) shows $P(N_{\text{occ}})$ of a system at low density, $\rho R_g^3 = 0.046$, i.e., well below $\tilde{\rho}_f$. Some small clusters are present but single dendrimers dominate: this system is a fluid of single dendrimers. Increasing the density to $\rho R_g^3 = 0.138$, Fig. 1(b), while still staying below $\tilde{\rho}_f$, we find that a distinctive distribution of larger clusters has also developed. The sizes of these clusters are not uniformly distributed; rather a single cluster size, $N_{\text{occ}}^{\text{pref}}$, is favored, in full agreement with theoretical predictions [20]. Here, the system forms a cluster fluid, as already studied

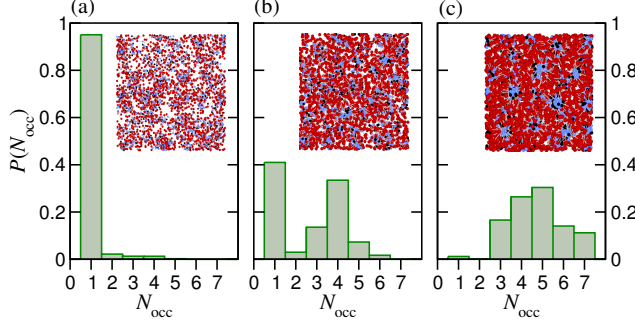


FIG. 1. Color online. The probability distribution $P(N_{\text{occ}})$ to find cluster size N_{occ} in (a) the fluid state at $\rho R_g^3 = 0.046$; (b) the cluster fluid state at $\rho R_g^3 = 0.138$; and (c) the solid state at $\rho R_g^3 = 0.323$. The insets show simulation snapshots, where clustering can be seen from the crowding of the dendrimers' core monomers [black and blue (light gray)]. Shell monomers are shown in red (dark grey). Monomers are not drawn to scale.

in detail in previous work, albeit for a different dendrimer model only showing clustering at higher occupancies than the present model [2, 26]. Finally, the density was increased above $\tilde{\rho}_f$ to the value $\rho R_g^3 = 0.323$, Fig. 1(c). Now, single dendrimers have almost completely vanished from the solution and have been replaced by clusters of a preferred occupation of $N_{\text{occ}}^{\text{pref}} = 4 - 5$. Visual inspection reveals that this system has spontaneously developed local crystalline order, albeit forming a distorted crystal. This finding is corroborated by an analysis of the radial distribution function of the clusters' centers of mass, which has developed a pronounced first peak centered at a value close to the predicted \tilde{a} and clearly separated from the second peak. System sizes, however, do not allow for a positive determination of a particular structure. Similar results were found for several other densities above $\tilde{\rho}_f$, proving that the cluster liquid is *unstable* in this density regime.

Spontaneous crystallization, however, does not provide information which crystalline structure is the one of lowest free energy; crystallites formed could exhibit the structure with the lowest barrier separating it from the fluid state [27, 28]. We therefore artificially prepared perfect bcc and fcc cluster crystals at various densities ρ , by placing $N_{\text{occ}} \gtrsim N_{\text{occ}}^{\text{pref}}(\rho)$ dendrimers per perfect lattice site and then delimited their range of mechanical stability by performing NVT- and NPT-Monte Carlo simulations. Non-stable crystals melted within a few simulation sweeps into diffusive fluids, as manifested by a steady increase of the dendrimers' mean-square displacement and an accompanying loss of the ordered structure. The

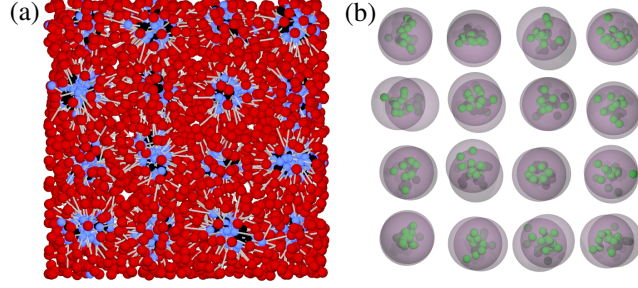


FIG. 2. Color online. Simulation snapshot of a fcc dendrimer cluster crystal of occupancy $N_{\text{occ}} = 10$ at $\rho R_g^3 = 0.438$. (a) A full-monomer representation of the crystal. Clustering can be seen from the crowding of core monomers [black and blue (light gray)]. (b) The dendrimers' centers of mass (small spheres) are found to 99% in the big, gray spheres around the cluster's centers of mass.

mechanically stable systems, however, remained in the crystalline, clustered arrangement throughout the whole simulation runs. Fig. 2(a) shows a typical simulation snapshot of a cluster crystal in the full-monomer representation of the dendrimers, where the clustering can be seen from the crowding of core monomers [black, blue (light gray)], which are surrounded by a cloud of shell monomers [red (dark gray); also cf. Fig. S1]. The clustering and the self-assembly of the clusters onto the lattice sites of a (fcc) crystal become even more evident when plotting just the dendrimers' centers of mass, Fig. 2(b), denoted there by small spheres. The irregular shapes of the various clusters are a manifestation of the instantaneous fluctuations of each dendrimer around its lattice site and show that the centers of mass of the individual dendrimers are not tightly bound to lie on top of each other. These findings are in full agreement with the theoretical picture, which predicts these oscillations to give rise to intra-cluster breathing modes that manifest themselves as optical branches in the phonon spectrum of the crystal [18]. We quantify these fluctuations by plotting gray spheres, centered around the clusters' centers of mass, and which contain the latter to a probability of 99%. Spheres from different lattice sites do not overlap, confirming the prediction that the clusters are well-localized around their lattice sites [20].

The results of the simulations delimiting the range of mechanical stability are summarized in Fig. 3, revealing that a large, insular part of density-occupancy space allows for the formation of mechanically stable cluster solids. The minimum density to provide mechanical stability of the cluster crystals is found to be $\rho R_g^3 \cong 0.225$, independently of the occupation number. While the determination of the precise location of the freezing density ρ_f is not

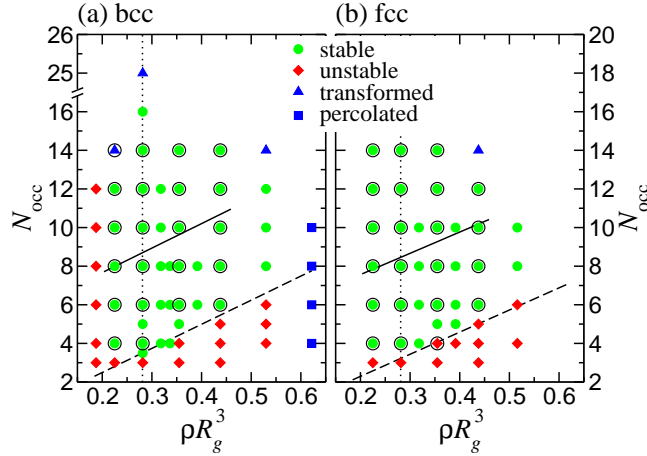


FIG. 3. Color online. The mechanical stability of dendrimer cluster crystals for (a) bcc and (b) fcc as function of density ρR_g^3 and occupation number N_{occ} . State points for which crystals remained stable are denoted by circles (\bullet), those where crystals melted as diamonds (\blacklozenge). The predicted freezing density $\tilde{\rho}_f$ is shown as vertical, dotted line at $\rho R_g^3 = 0.281$. For high occupations and densities, systems transformed (\blacktriangle) or formed percolated networks (\blacksquare) (see text). Systems for which the free energy was measured are circled in black. The dashed line plots the theoretical prediction $\tilde{N}_{\text{occ}}(\rho)$, while the equilibrium occupation $N_{\text{occ}}^{\text{eq}}(\rho)$ (see text) is plotted as solid line.

the subject of this paper, these results demonstrate that $\rho_f \simeq \tilde{\rho}_f$.

As can be seen in Fig. 3, the minimum occupation number leading to mechanically stable solids increases linearly with density for both bcc and fcc. Systems with the lowest stable occupation, $N_{\text{occ}} \simeq 4$ showed single events of lattice site hopping and subsequent healing of the resulting defect. However, due to the limited time-scales accessible in our simulations and the crowded systems studied, complex structural rearrangements and hopping events leading to long-time diffusion [14, 15] have not been observed frequently. Crystals of high occupations, $N_{\text{occ}} \simeq 14$, further remained mechanically stable upon artificially introducing lattice defects like single clusters of lower occupancy, or even lattice vacancies or interstitials. Also mixed occupations, where not every lattice site was occupied by the same amount of dendrimers, remained stable, provided the average value of N_{occ} was chosen from the island of stability (see Fig. 3), in full agreement with the theoretical prediction of cluster polydispersity in the crystal [14, 20].

Crystals with even higher occupations, i.e., $N_{\text{occ}} \gtrsim 16$ were not found to be stable: they

transformed to distorted crystal structures of lower occupations by splitting clusters and halving the lattice constant, thereby taking these crystals back to the island of stability (Fig. 3, triangles). This shows the propensity of over-occupied crystals to adjust their occupancy towards an optimal value, a feature which will be confirmed quantitatively by free energy calculations in what follows. At high densities and rather low occupations, the lattice spacing accordingly shrinks and enters the length regime of the bonds between the dendrimers' monomers. Here, the crystalline arrangement of well-defined clusters also cannot be sustained: dendrimers stretch and are shared between two clusters, leading to disordered percolated networks of dendrimers (Fig. 3, squares). This phenomenon reflects that at such high densities the effective pair potential picture, which predicts an unlimited growth of cluster occupancy with density, $N_{\text{occ}} \propto \rho$, breaks down *qualitatively* since steric crowding between the monomers prevents further cluster growth upon sufficient compression.

Having established the existence of a broad region of their *mechanical* stability, it is pertinent to assess the crystals' *thermodynamic* stability and their optimal occupation at given density. To this end, we calculated the excess free energy per particle $\beta f_{\text{ex}} = \beta F_{\text{ex}}/N$ for the mechanically stable crystals with the help of thermodynamic integration as outlined in Refs. [6, 16]. Here, the reference state is chosen as non-interacting dendrimers confined to the desired crystal structure by potential wells. Being the same for all crystal structures, the reference free energy $\beta F_{\text{id}}/N$ may be disregarded. Measuring βf_{ex} for several values of N_{occ} at given crystal structure and fixed density, we determine the equilibrium occupancy $N_{\text{occ}}^{\text{eq}}$ as the one that minimizes the free energy, see Fig. 4(a) [19]. In qualitative agreement with theoretical predictions, $N_{\text{occ}}^{\text{eq}}$ increases linearly with density, Fig. 4(b). However, there exist quantitative deviations between the two, manifesting the role of the many-body interactions. Whereas the pair-potential description predicts $N_{\text{occ}} \propto \rho$, here there is a non-zero offset d , $N_{\text{occ}} = c\rho + d$. At freezing, the optimal occupation number from the monomer-resolved simulations turns out to be *higher* than theoretically predicted. This indicates that the many-body interactions, whose importance grows with occupancy, have the effect of strengthening the overall attractions between the soft particles at close approach. Since these properties are model-specific, we do not attempt a more detailed analysis here. However, we point out that the theoretical prediction of $\tilde{N}_{\text{occ}}(\rho)$ is found to be an excellent estimate for the lower limit in occupancy of mechanically stable crystals (see Fig. 3). Indeed, these occupancies are sufficiently low for pair potentials to still be approximately valid, their degree of validity

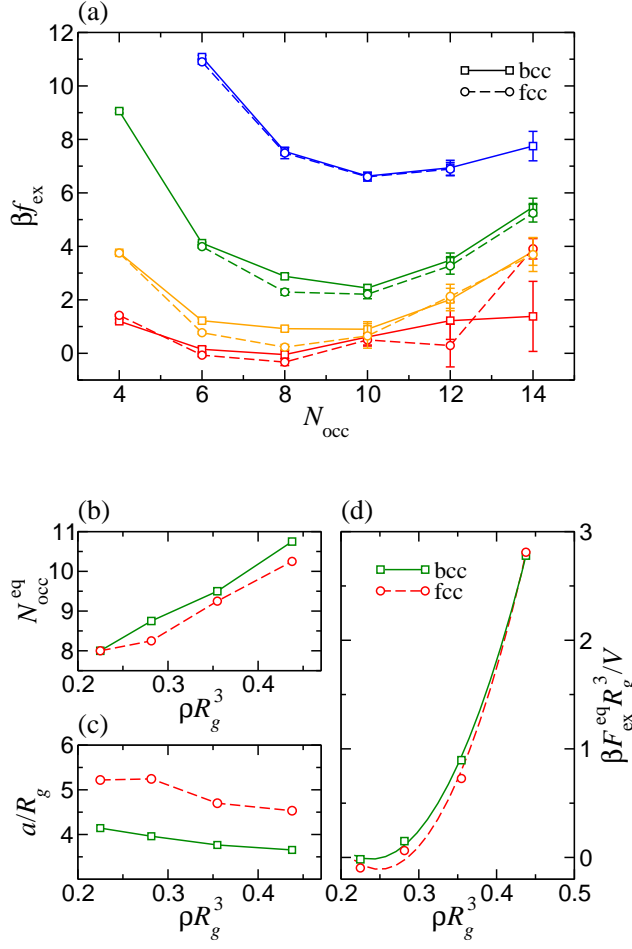


FIG. 4. Color online. All data is plotted for fcc (o) and bcc (\square) lattices. (a) The free energy per dendrimer, βf_{ex} , as a function of N_{occ} at different densities, from bottom to top: $\rho R_g^3 = 0.22, 0.28, 0.36$ and 0.44 , showing for each density a different optimal occupancy, $N_{\text{occ}}^{\text{eq}}$, that minimizes it. (b) The equilibrium occupancy, $N_{\text{occ}}^{\text{eq}}$, as function of density ρR_g^3 . (c) The equilibrium lattice constant a/R_g shrinks with increasing density. (d) The equilibrium free energy per volume, $\beta F_{\text{ex}}^{\text{eq}} R_g^3 / V$ as a function of the density ρ , evaluated at the equilibrium occupancy $N_{\text{occ}}^{\text{eq}}(\rho)$. Fcc is found to be the thermodynamically stable crystal.

diminishing as N_{occ} grows. In Fig. 4(d) we show the free energy per volume of the equilibrium crystals as a function of density. We find that the fcc crystals have a slightly lower free energy than bcc for all densities considered.

In contrast to amphiphilic dendrimers, ring polymers cannot form cluster crystals due to their drastic shrinkage upon compression [8]. It is therefore pertinent to study the conforma-

tions of dendrimers in the clusters of the thermodynamically stable crystals. The radius of gyration of the dendrimers shows little variation with density, due to the necessary balance between the exterior and interior osmotic pressure of clusters and the constraints imposed by the regularly branched dendritic architecture. Nevertheless, the configurations of the dendrimers change considerably upon increasing density, a fact manifested by a density-dependence of the most probable distance of shell monomers from their dendrimer’s center of mass. While shell monomers can backfold to the dendrimer’s core at low densities, the cluster formation at finite densities increasingly forces the shell monomers to move to the rim of the molecules [29].

Altogether, the cluster crystals discovered in our study are characterized by a hierarchy of self-organization at various interconnected levels. First, the individual dendrimers adjust their conformations to the thermodynamic conditions; second, the individual clusters adjust their population and are thus robust against cluster polydispersity and crystal defects; and finally at the macroscopic level, the flexibility of the cluster crystals is manifested through the mechanism of restructuring of non-optimally occupied cluster crystals, the hopping of dendrimers among crystal sites, and the adjustment of the associated lattice constant. Discrepancies between the fully microscopic and the effective potential pictures exist due to the fact that the strong steric repulsions of the monomers prohibit the *ad libitum* growth of the clusters’ population. Still, the salient features of soft cluster crystals have been confirmed. The range of stability of these structures is sufficiently broad to render them into materials of practical as well as fundamental importance.

In summary, we have shown at a microscopic level that cluster crystals exist in suitably synthesized soft matter systems. More detailed computational investigations in both the effective and the microscopical description will be needed to uncloak the whole beauty of these intriguing systems and understand, for example, the nucleation of soft cluster crystals or the transformations of dendrimer crystals at high occupations and densities; this will be the topic of future investigations. Our results convey the clear message that an experimental realization of cluster crystals employing simple and easy to synthesize dendritic macromolecules is possible. We thereby provide guidelines to achieve this goal, which will lead to the production of a new class of materials with most intriguing physical properties.

We thank Daan Frenkel (Cambridge) for helpful discussions. D.A.L. thanks the Wolfgang Pauli Institute. B.M.M. acknowledges the MFPL VIPS program (funded by BMWF and the

City of Vienna), and EU funding (FP7-PEOPLE CIG-2011 No. 303860). Partial support by the ITN-COMPLOIDS (Grant Agreement No. 234810) and computer time at the Vienna Scientific Cluster are gratefully acknowledged.

-
- [1] W. Klein, H. Gould, R. A. Ramos, I. Clejan, and A. I. Mel'cuk, *Physica A* **205**, 738 (1994).
 - [2] C. N. Likos, A. Lang, M. Watzlawek, and H. Löwen, *Phys. Rev. E* **63**, 031206 (2001).
 - [3] B. M. Mladek, D. Gottwald, G. Kahl, M. Neumann, and C. N. Likos, *Phys. Rev. Lett.* **96**, 045701 (2006).
 - [4] F. Sciortino, S. Mossa, E. Zaccarelli, and P. Tartaglia, *Phys. Rev. Lett.* **93**, 055701 (2004).
 - [5] H. Sedgwick, K. Kroy, A. Salonen, M.B. Robertson, S.U. Egelhaaf, and W.C.K. Poon, *Eur. Phys. J. E* **16**, 77 (2005).
 - [6] B. M. Mladek, P. Charbonneau, C. N. Likos, D. Frenkel, and G. Kahl, *J. Phys.: Condens. Matter* **20**, 494245 (2008).
 - [1] B. M. Mladek, G. Kahl, and C. N. Likos, *Phys. Rev. Lett.* **100**, 028301 (2008).
 - [8] A. Narros, A. J. Moreno, and C. N. Likos, *Soft Matter* **6**, 2435 (2010).
 - [2] D. A. Lenz, B. M. Mladek, C. N. Likos, G. Kahl, and R. Blaak, *J. Phys. Chem. B* **115**, 7218 (2011).
 - [10] M. O. Goerbig, P. Lederer, and C. Morais Smith, *Phys. Rev. B* **68**, 241302 (2003).
 - [11] N. Cooper, *Adv. Phys.* **57**, 539 (2008).
 - [12] S. Saccani, S. Moroni, and M. Boninsegni, *Phys. Rev. B* **83**, 092506 (2011).
 - [13] S. Saccani, S. Moroni, and M. Boninsegni, *Phys. Rev. Lett.* **108**, 175301 (2012).
 - [14] A. J. Moreno and C. N. Likos, *Phys. Rev. Lett.* **99**, 107801 (2007).
 - [15] D. Coslovich, L. Strauss, and G. Kahl, *Soft Matter* **7**, 2127 (2011).
 - [16] B. M. Mladek, P. Charbonneau, and D. Frenkel, *Phys. Rev. Lett.* **99**, 235702 (2007).
 - [17] A. Nikoubashman, G. Kahl, and C. N. Likos, *Soft Matter* **7**, 4121 (2012).
 - [18] T. Neuhaus and C. N. Likos, *J. Phys.: Condens. Matter* **23**, 234112 (2011).
 - [19] K. Zhang, P. Charbonneau, and B. M. Mladek, *Phys. Rev. Lett.* **105**, 245701 (2010).
 - [20] C. N. Likos, B. M. Mladek, D. Gottwald, and G. Kahl, *J. Chem. Phys.* **126**, 224502 (2007).
 - [21] J. Dautenhahn and C. K. Hall, *Macromolecules* **27**, 5399 (1994).
 - [22] A. A. Louis, P. G. Bolhuis, J. P. Hansen, and E. J. Meijer, *Phys. Rev. Lett.* **85**, 2522 (2000).

- [23] B. Capone, J.-P. Hansen, and I. Coluzza, *Soft Matter* **6**, 6075 (2010).
- [24] Note1, see Supplemental Material for details on the dendrimer model chosen here.
- [25] Note2, see Supplemental Material (Fig. S1) for the general shape of the effective interactions of amphiphilic dendrimers.
- [26] D. A. Lenz, B. M. Mladek, C. N. Likos, and R. Blaak, (to be published).
- [27] S. Alexander and J. McTague, *Phys. Rev. Lett.* **41**, 702 (1978).
- [28] R. A. Van Santen, *J. Phys. Chem.* **88**, 5768 (1984).
- [29] Note3, see Supplemental Material for details on this behavior.

Supplemental Material for paper: Microscopically-resolved simulations prove the existence of soft cluster crystals

Dominic A. Lenz, Ronald Blaak, Christos N. Likos, and Bianca M. Mladek

THE DENDRIMER MODEL

A generic view of the amphiphilic dendrimer architecture, of the effective pair potential and of the hierarchical assembly of the molecules into a cluster crystal is shown in Fig. S1. We employ the dendrimer model already introduced before in Refs. [1, 2] and based on Ref. [3]. We study amphiphilic dendrimers of second generation which have two central monomers. The dendrimers' 14 monomers are divided into two classes: the eight monomers of the outermost generation ($g = 2$) form the solvophilic shell of the dendrimer (index S), and all monomers of the interior generations ($g = 0$ and $g = 1$) form the solvophobic core (index C), resulting in amphiphilic dendrimers. Interactions between any two monomers, separated by a distance r are modeled by a Morse potential [3], which is given by

$$\beta\Phi_{\mu\nu}^{\text{Morse}}(r) = \epsilon_{\mu\nu} \left\{ \left[e^{-\alpha_{\mu\nu}(r-\sigma_{\mu\nu})} - 1 \right]^2 - 1 \right\}, \quad \mu\nu = \text{CC, CS, SS} \quad (1)$$

where $\sigma_{\mu\nu}$ denotes the effective diameter between two monomers of species μ and ν . All energy scales employed are measured in units of $\beta = (k_B T)^{-1}$, with T being the temperature and k_B Boltzmann's constant. The Morse potential is characterized by a repulsive short-range behavior and an attractive part at long distances, whose depth and range are parametrized via $\epsilon_{\mu\nu}$ and $\alpha_{\mu\nu}$, respectively. The core monomer diameter σ_c is chosen to be the unit of length for the model parameters given in Tab. I.

The bonds between adjacent monomers of relative distance r are modeled by the finitely extensible nonlinear elastic (FENE) potential, given by

$$\beta\Phi_{\mu\nu}^{\text{FENE}}(r) = -K_{\mu\nu} R_{\mu\nu}^2 \log \left[1 - \left(\frac{r - l_{\mu\nu}}{R_{\mu\nu}} \right)^2 \right], \quad \mu\nu = \text{CC, CS} \quad (2)$$

where the spring constant $K_{\mu\nu}$ restricts the monomer separation to be within a distance $R_{\mu\nu}$ from the equilibrium bond length $l_{\mu\nu}$.

We simulated more than 100 different realizations of dendrimers, determining the zero-density pair interactions via the algorithm outlined in [4]. We then chose the dendrimer

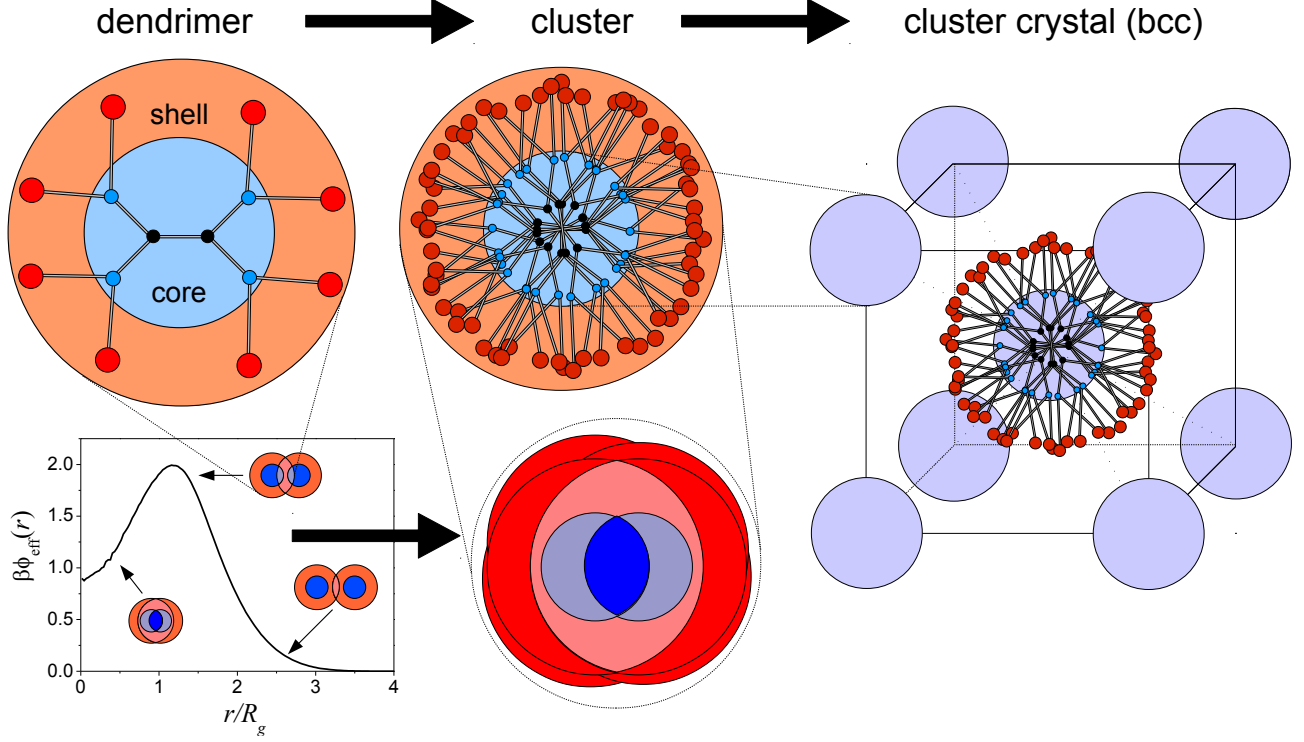


FIG. S1. Schematic representation of amphiphilic dendrimers of second generation, consisting of a solvophobic core (black and blue inner monomers) and a solvophilic shell (red outer monomers; monomers not drawn to scale). Several, interpenetrating dendrimers form clusters, which is expected to be promoted by the dendrimer-dendrimer interaction, $\Phi_{\text{eff}}(r)$ (bottom left), which favors clustering. Clusters can then freeze into crystals. Here, $\beta = (k_B T)^{-1}$ and R_g is the infinite dilution radius of gyration.

with the deepest minimum in Fourier transform, which promises a high ability of clustering. Its parameters are given in Tab. I.

We stress that we also carried out simulations of cluster crystals for other realizations of dendrimers, whose effective interactions are far less promising regarding their clustering behavior. While these systems are more difficult to access computationally due to their higher necessary equilibrium occupancies, the obtained results are in full accordance with the findings presented in the main part of the present contribution.

Morse	ϵ	$\alpha\sigma_c$	σ/σ_c
CC	0.714	1.8	1.0
CS	0.01785	6.0	1.75
SS	0.01785	6.0	2.5
FENE	$K\sigma_c^2$	l_0/σ_c	R/σ_c
CC ($g = 0$)	60	3.1875	0.6375
CC ($g \neq 0$)	60	1.875	0.375
CS	30	3.5625	0.7125

TABLE I. Potential parameters of the dendrimer considered in this study. The radius of gyration of an isolated dendrimer is $R_g = 3.589\sigma_c$.

DENDRIMER STRUCTURE IN THE CLUSTER CRYSTALS

In the main text, we refer to the adjustment of dendrimer sizes and conformations upon changes of the density ρ and the cluster occupation N_{occ} . Here we show quantitative evidence of this effect. The dependence of the dendrimers' radii of gyration on ρ and N_{occ} , $R_g(\rho; N_{\text{occ}})$, for the mechanically stable crystals in (cf. Fig. 3 of main text) is shown in Fig. S2. For reference, the zero-density value R_g is plotted as well. The equilibrium values of the radii of gyration $R_g^{\text{eq}}(\rho)$, corresponding to the optimal occupancy $(\rho, N_{\text{occ}}^{\text{eq}})$ according to Fig. 4 are displayed by the open symbols, revealing that their values are nearly density-independent and, interestingly enough, very close to the zero density value. The dependence of the dendrimer size on N_{occ} for a fixed density ρ is a monotonically increasing function, a feature that can be understood through the influence of two interconnected mechanism. On the one hand, as N_{occ} grows, the dendrimers have to stretch to accommodate the increasing number of monomers. On the other, the concomitant increase of the lattice constant brings the neighbors further apart and therefore it slows down the growth of the repulsions from the neighboring dendrimers, which have the tendency of shrinking the molecules. The insensitivity of the equilibrium value to the density can be understood in terms of an equality of the osmotic pressure from the interior of the clusters, Π_{int} , and that from the neighboring clusters, Π_{ext} . As both scale proportionally to N_{occ} and the lattice constant is

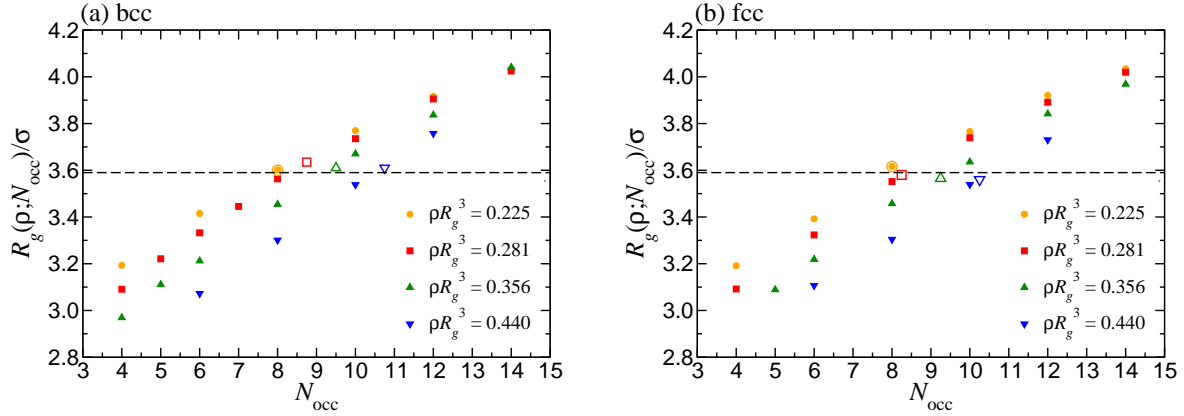


FIG. S2. The radius of gyration of (a) bcc and (b) fcc crystals as a function of crystal occupation number for various crystal densities as indicated in the legends. The open symbols denote the value of $R_g(\rho; N_{\text{occ}})$ at the optimal occupation number, obtained by thermodynamic integration as described in the main text, and they are color- and symbol coded as the filled symbols. The horizontal line indicates the value $R_g = 3.59\sigma$ of the gyration radius of the dendrimers at infinite dilution.

rather insensitive to the density, this quantity cancels out from both sides of the equation, bringing about the aforementioned insensitivity of R_g on ρ . This rigidity of the dendrimers with respect to strong deformations lies at stark contrast to the behavior of linear or ring-shaped polymer chains, which shrink above their overlap density ρ^* according to the law $R_g(\rho)/R_g = (\rho/\rho^*)^{-1/8}$.

The fact that $R_g(\rho)$ turns out to be also almost identical to its zero-density value does not imply, however, that the *conformation* of the dendrimer is invariant with density. In Fig. S3, the monomer density profiles with respect to the dendrimer's center or mass in cluster crystals are shown. In particular, in Fig. S3(a) the profiles of the core monomers ($g = 0$ and $g = 1$) are compared for several occupations N_{occ} at fixed density $\rho R_g^3 = 0.282$, including the profiles for the equilibrium occupancy, $N_{\text{occ}}^{\text{eq}} \cong 8$; as a reference, the profile of an isolated dendrimer is also plotted. The same comparison is shown for the shell monomers ($g = 2$) in Fig. S3(b). We find that for all finite-density profiles, and in contrast to the case of the isolated dendrimer, the back-folding of shell monomers to the center of the dendrimer is suppressed due to the presence of core monomers of other dendrimers which occupy the available space. Further, increasing the occupancy naturally leads to an increasing spatial

extension of the core-monomer aggregate as well as an increased lattice constant. Thus, the shell monomer distribution broadens for increasing occupancy, and the maximum probability distance moves slightly towards the exterior of dendrimers. It can be seen that the profiles of the equilibrium system ($N_{\text{occ}}^{\text{eq}} \cong 8$) and of an isolated dendrimer differ significantly from one another, while their radii of gyration were found to almost coincide. This equality originates in two opposing effects, namely a reduced probability of finding shell monomers within the dendrimer center at finite densities, paired with an increased probability of finding core monomers at the center.

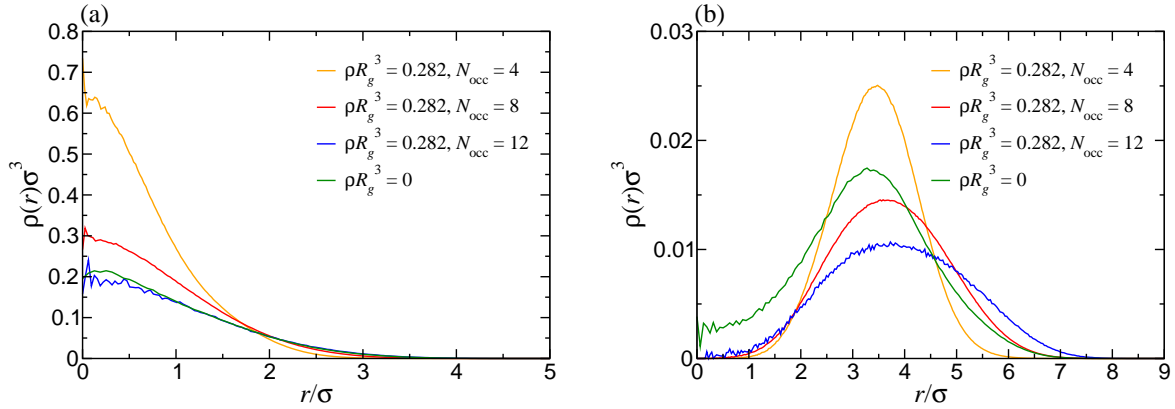


FIG. S3. Comparison of the monomer density profiles of dendrimers in the cluster fcc-solid for fixed density ρ and varying occupancy N_{occ} , as indicated in the legend. As a reference, the monomer profiles of isolated amphiphilic dendrimers ($\rho R_g^3 = 0$) are also shown. (a) Core profiles; (b) Shell profiles.

-
- [1] B. M. Mladek, G. Kahl, and C. N. Likos, Phys. Rev. Lett. **100**, 028301 (2008).
 - [2] D. A. Lenz, B. M. Mladek, C. N. Likos, G. Kahl, and R. Blaak, J. Phys. Chem. B **115**, 7218 (2011).
 - [3] P. Welch and M. Muthukumar, Macromolecules **31**, 5892 (1998).
 - [4] B. M. Mladek and D. Frenkel, Soft Matter **7**, 1450 (2011).